Supplemental Figure 1. Topological distribution of CD44+ and CD24+ cells in breast tumors. A representative example of a HER2+ invasive ductal breast carcinoma (T2) demonstrating different distribution of CD44+ and CD24+ cells in four selected areas in different parts of the tumor.

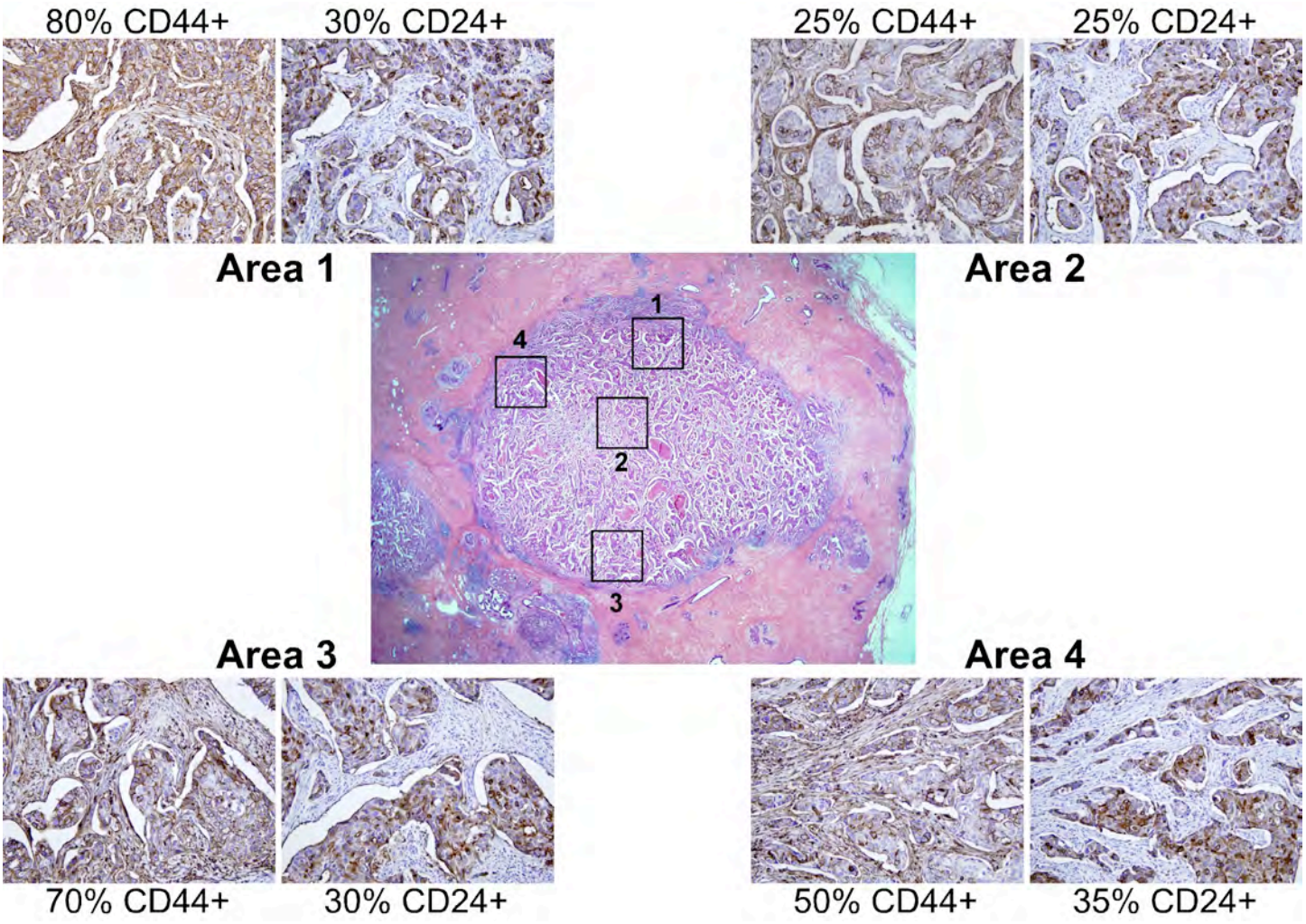

Supplemental Figure 2. Topological diversity of CD24+ and CD44+ cells in breast tumors. Graph shows the frequency of CD44+ (red) and CD24+ (blue) cells in four independent quadrants of each tumor. Cell frequencies were identified by immunohistochemistry (see Supplemental Figure 1 and Supplemental Table 2). The first row shows HER2+ tumors, the second row luminal A tumors, and the third row basal-like tumors.

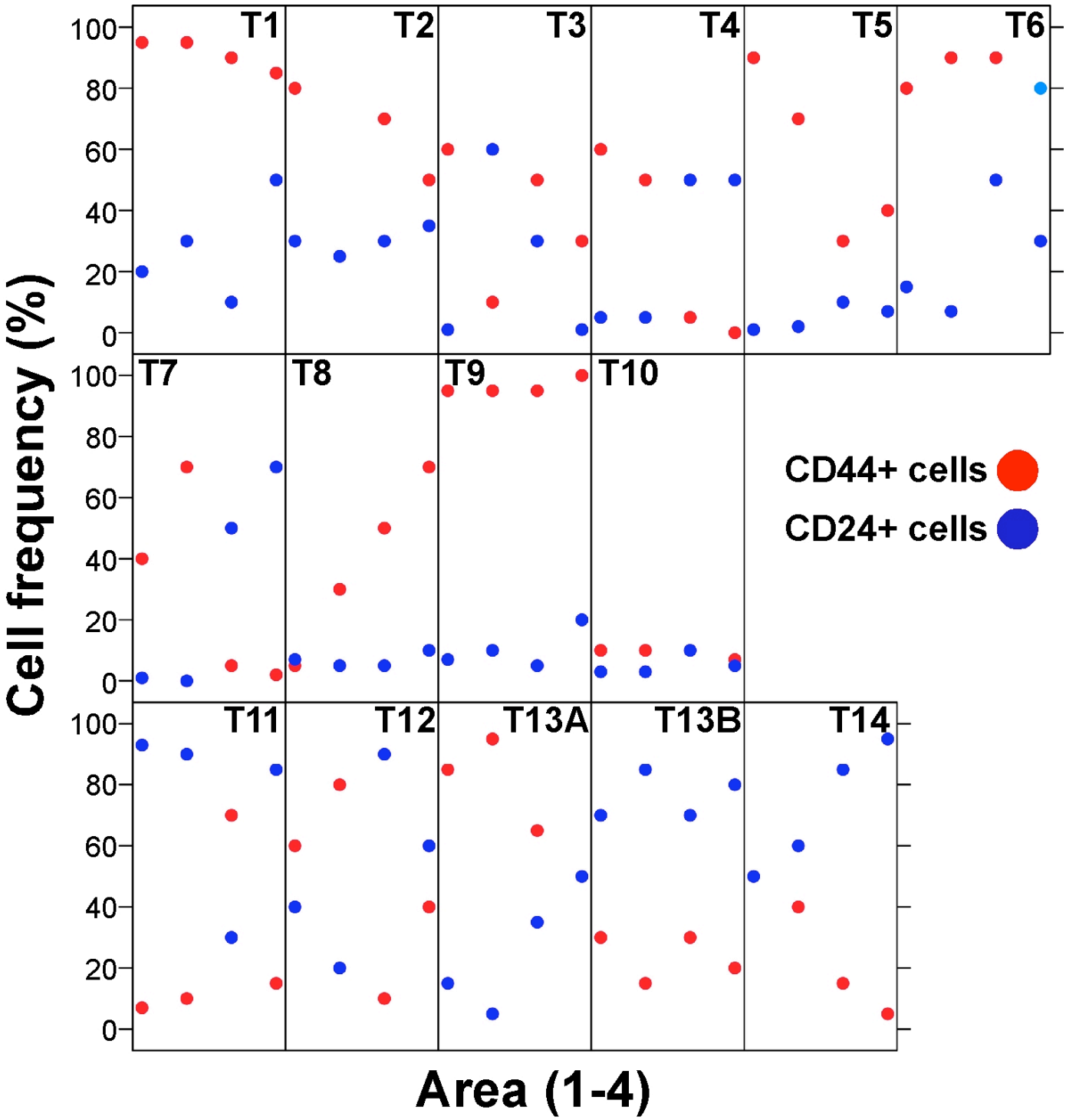

Supplemental Figure 3. Intra-tumor heterogeneity assessed by iFISH in tumor 14. (**A**) Immunohistochemical staining revealed heterogeneous expression of CD44 in selected areas in a basal-like breast cancer (T14). (**B**) iFISH analyses using BAC RP11-621K8 mapped to 8q24.13 (red) and chromosome 8 centromeric probe (green). CD44+ and CD44- tumor cells showed variable copy numbers of the 8q24.13 locus, mostly associated with polysomy of chromosome 8. (**C**) iFISH analyses using CD44 antibody (blue), BAC RP11-911J12 mapped to 12p13.1-12.3 (red dot) and chromosome 12 centromeric probe (green dot). Both CD44+ and CD44- tumor cells revealed increased copy number for 12p13.1-12.3 locus related to polysomy of chromosome12. Faint green is background autofluorescence. Scale bar: 10μ, magnification: 400x (immunohistochemistry) and 600x (iFISH).

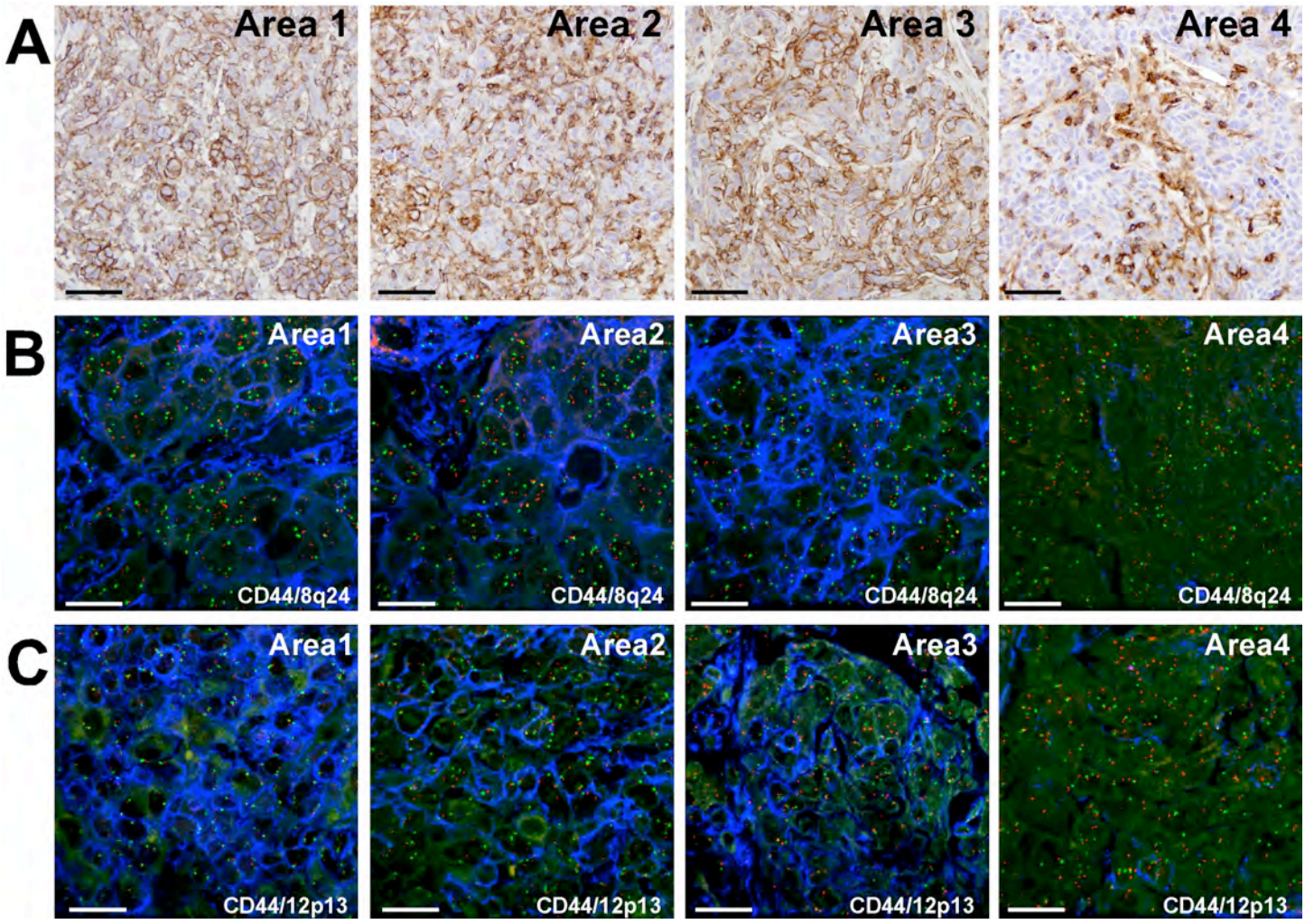

Supplemental Figure 4. Diversity of copy numbers in normal breast tissue samples. Shannon index depicting diversity within normal cell populations for each of the BACs/chromosomal regions analyzed in the study. Normal stromal cells surrounding the tumor cells were counted and their diversity scores calculated. Higher score indicates higher diversity. Diversity in normal cells was low and equal for all regions.

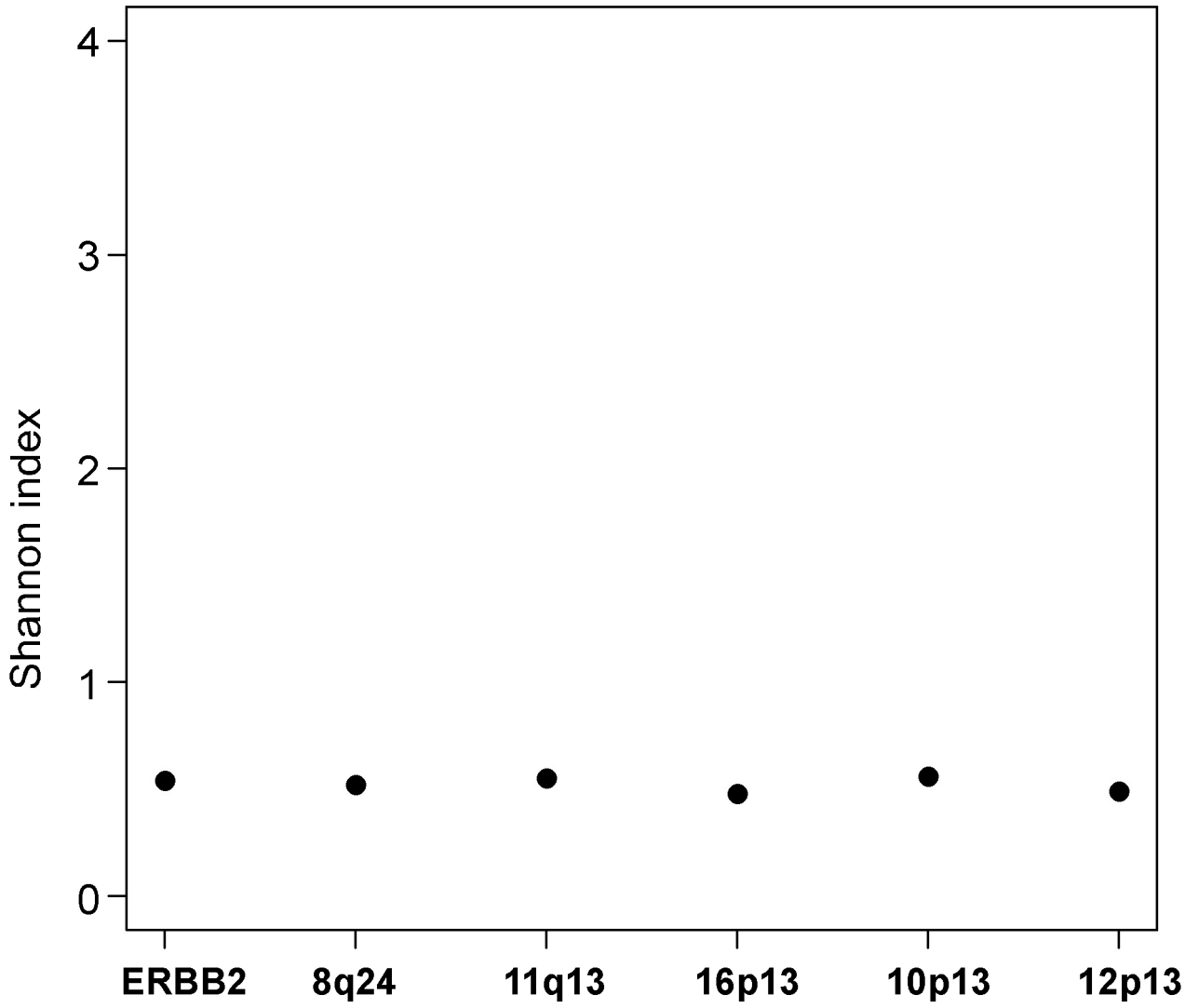

Supplemental Figure 5. Diversity of 1q32 copy number in HER2+ breast tumors. (**A**) Box plot depicting the distribution of 1q32 copy number gain defined as the number of signal observed for the 1q32 specific probe in 100 individual cells in each of the four indicated tumor cell subpopulations. The chromosome 1 centromeric probe gave a weak signal and could not be accurately counted. Differences are seen between cell populations and also progression stages both for median copy number gain as well as for range of distribution. (**B**) Histograms and kernel density estimates depicting the distribution of cells with the indicated copy number ratio. (**C**) Shannon index depicting diversity within tumor cell subpopulations and tumors. Higher score indicates higher diversity. (**D**) Simpson's index depicting diversity within tumor cell subpopulations and tumors. Higher score indicates higher diversity. (**E**) Rank-abundance (Whittaker) plots depicting the abundance of unique cancer cells.

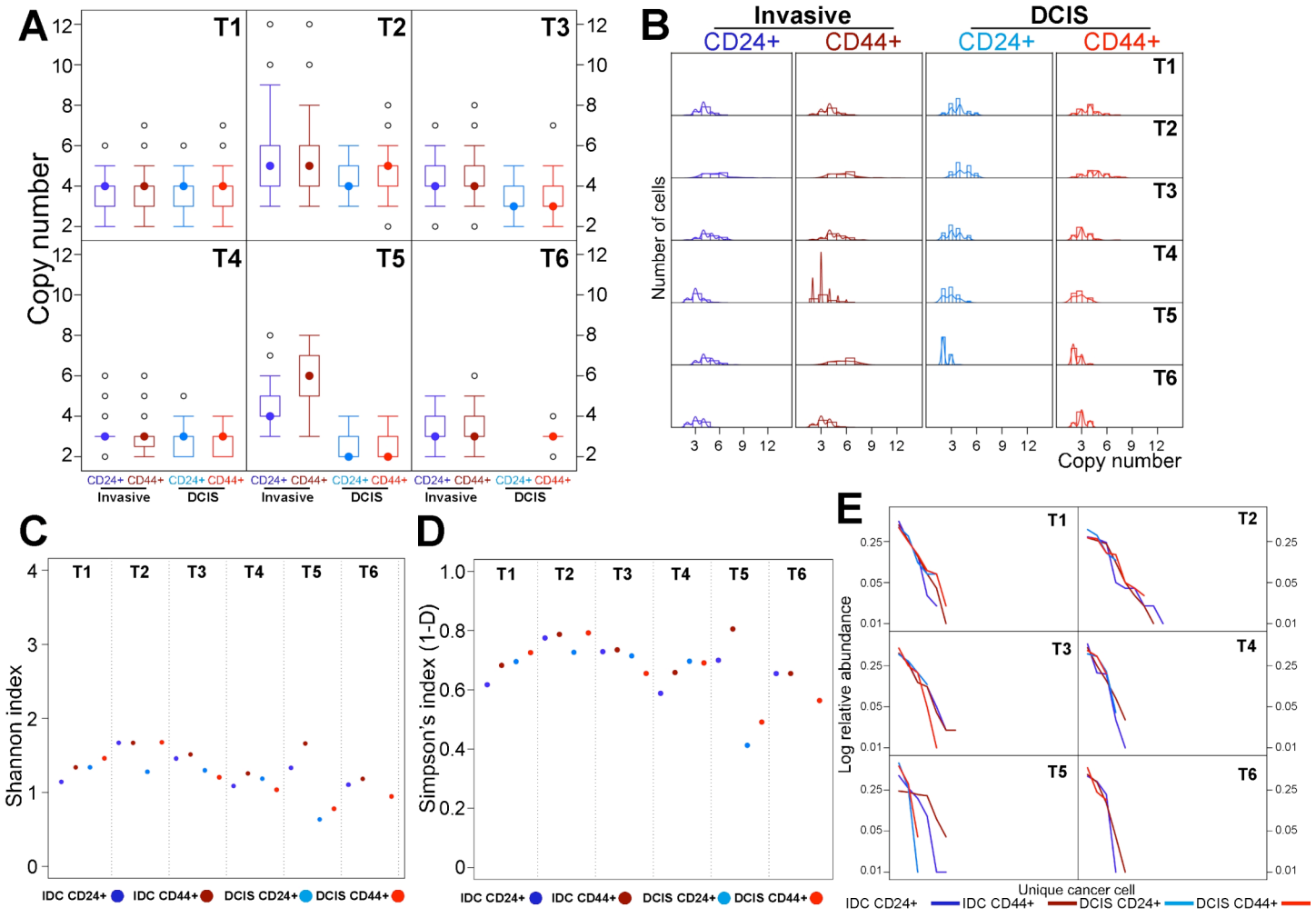

Supplemental Figure 6. Diversity of 10p13 copy number in basal-like breast tumors. (**A**) Box plot depicting the distribution of 10p13 copy number gain defined as the ratio of signal observed for the 10p13 specific and centromeric probes in 100 individual cells in each of the four indicated tumor cell subpopulations. Differences are seen between cell populations and also progression stages both for median copy number gain as well as for range of distribution. (**B**) Histograms and kernel density estimates depicting the distribution of cells with the indicated copy number ratio. (**C**) Shannon index depicting diversity within tumor cell subpopulations and tumors. Higher score indicates higher diversity. (**D**) Simpson's index depicting diversity within tumor cell subpopulations and tumors. Higher score indicates higher diversity. (**E**) Rank-abundance (Whittaker) plots depicting the abundance of unique cancer cells.

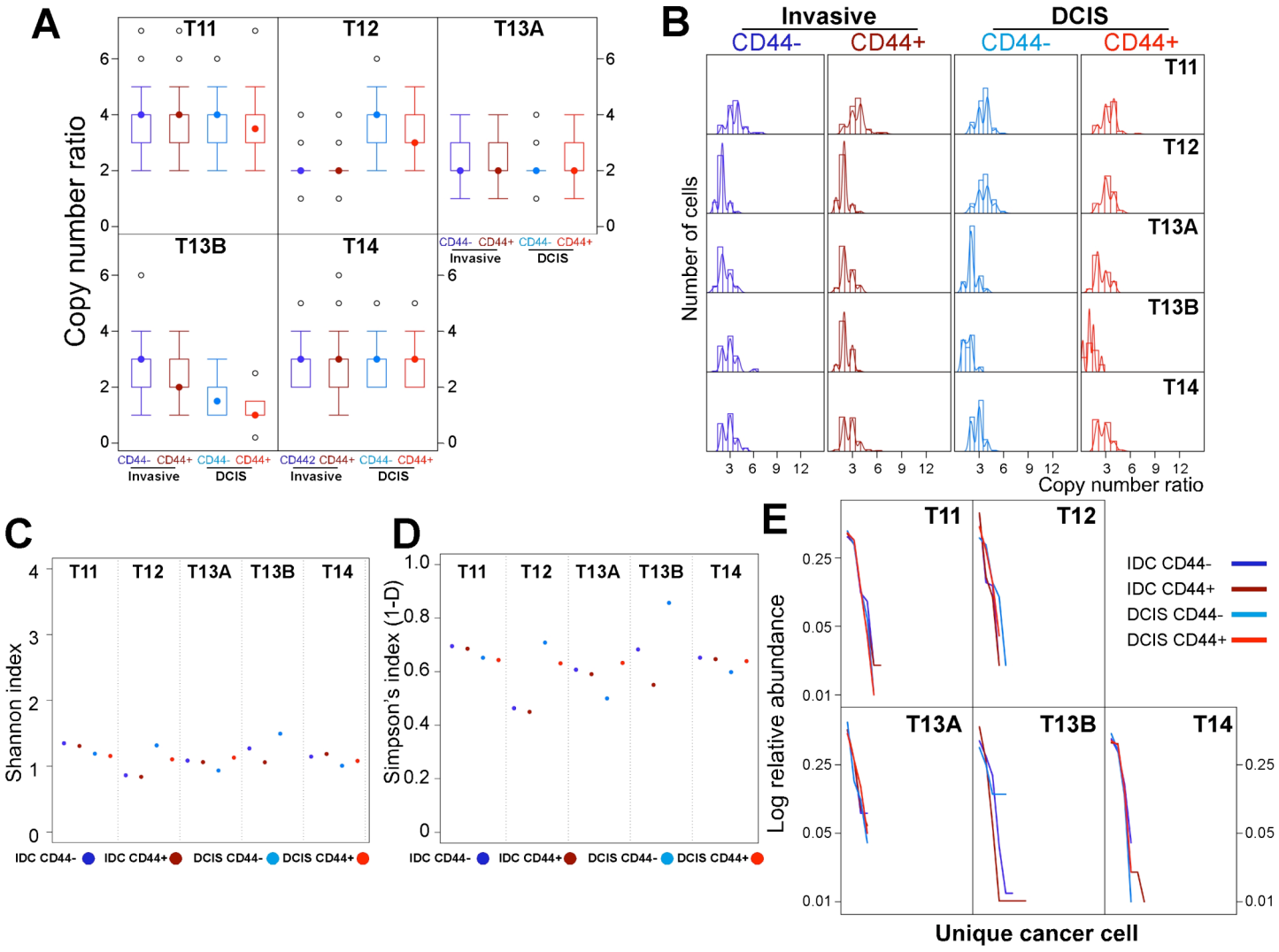

Supplemental Figure 7. Diversity of 11q13 copy number in luminal A breast tumors. (**A**) Box plot depicting the distribution of 11q13 copy number gain defined as the ratio of signal observed for the 11q13 -specific and centromeric probes in 100 individual cells in each of the four indicated tumor cell subpopulations. Differences are seen between cell populations and also progression stages both for median copy number gain as well as for range of distribution. (**B**) Histograms and kernel density estimates depicting the distribution of cells with the indicated copy number ratio. (**C**) Shannon index depicting diversity within tumor cell subpopulations and tumors. Higher score indicates higher diversity. (**D**) Simpson's index depicting diversity within tumor cell subpopulations and tumors. Higher score indicates higher diversity. (**E**) Rank-abundance (Whittaker) plots depicting the abundance of unique cancer cells.

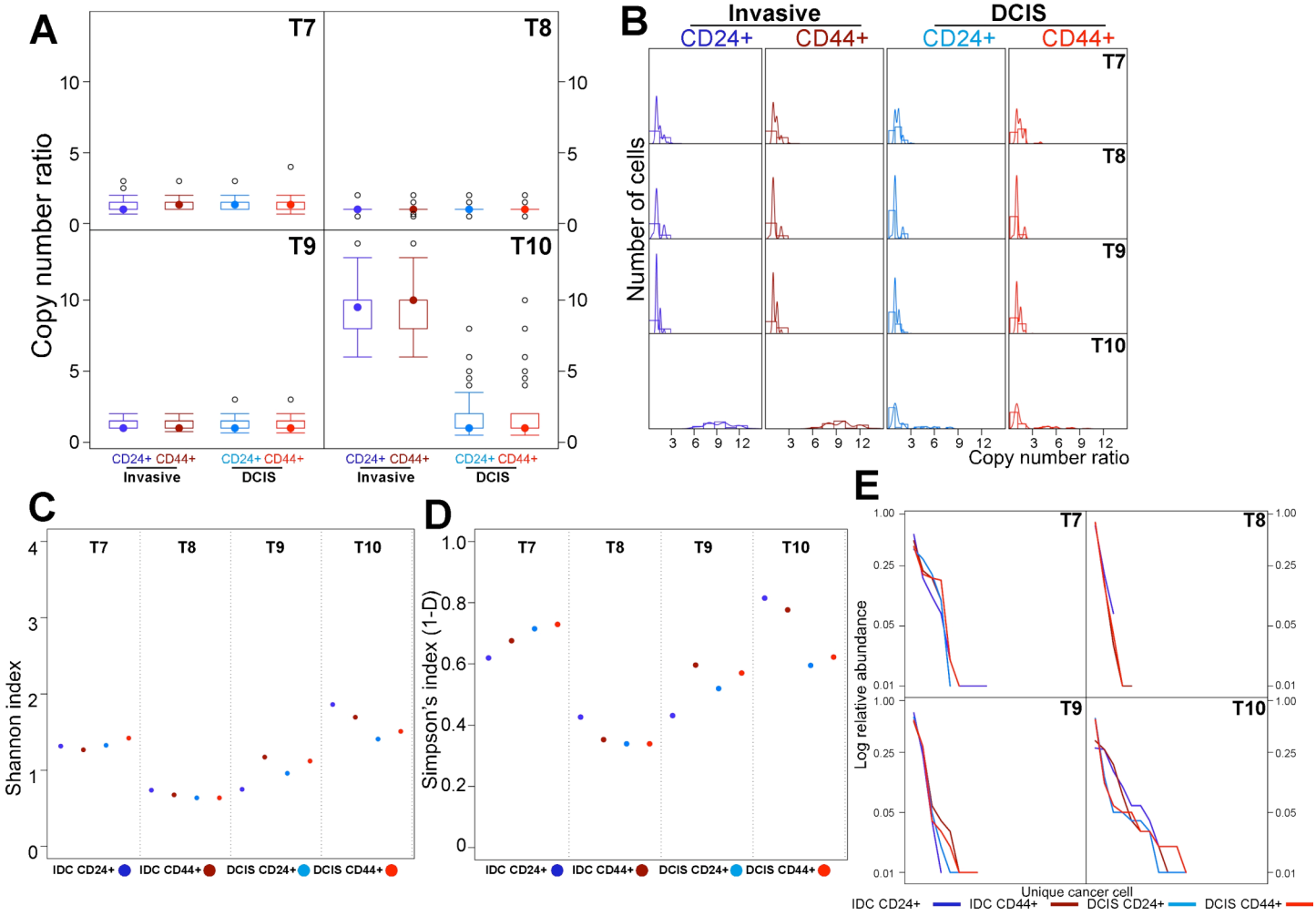

Supplemental Figure 8. Diversity of 12p13 copy number in basal-like breast tumors. (**A**) Box plot depicting the distribution of 12p13 copy number gain defined as the ratio of signal observed for the 12p13 -specific and centromeric probes in 100 individual cells in each of the four indicated tumor cell subpopulations. Differences are seen between cell populations and also progression stages both for median copy number gain as well as for range of distribution. (**B**) Histograms and kernel density estimates depicting the distribution of cells with the indicated copy number ratio. (**C**) Shannon index depicting diversity within tumor cell subpopulations and tumors. Higher score indicates higher diversity. (**D**) Simpson's index depicting diversity within tumor cell subpopulations and tumors. Higher score indicates higher diversity. (**E**) Rank-abundance (Whittaker) plots depicting the abundance of unique cancer cells.

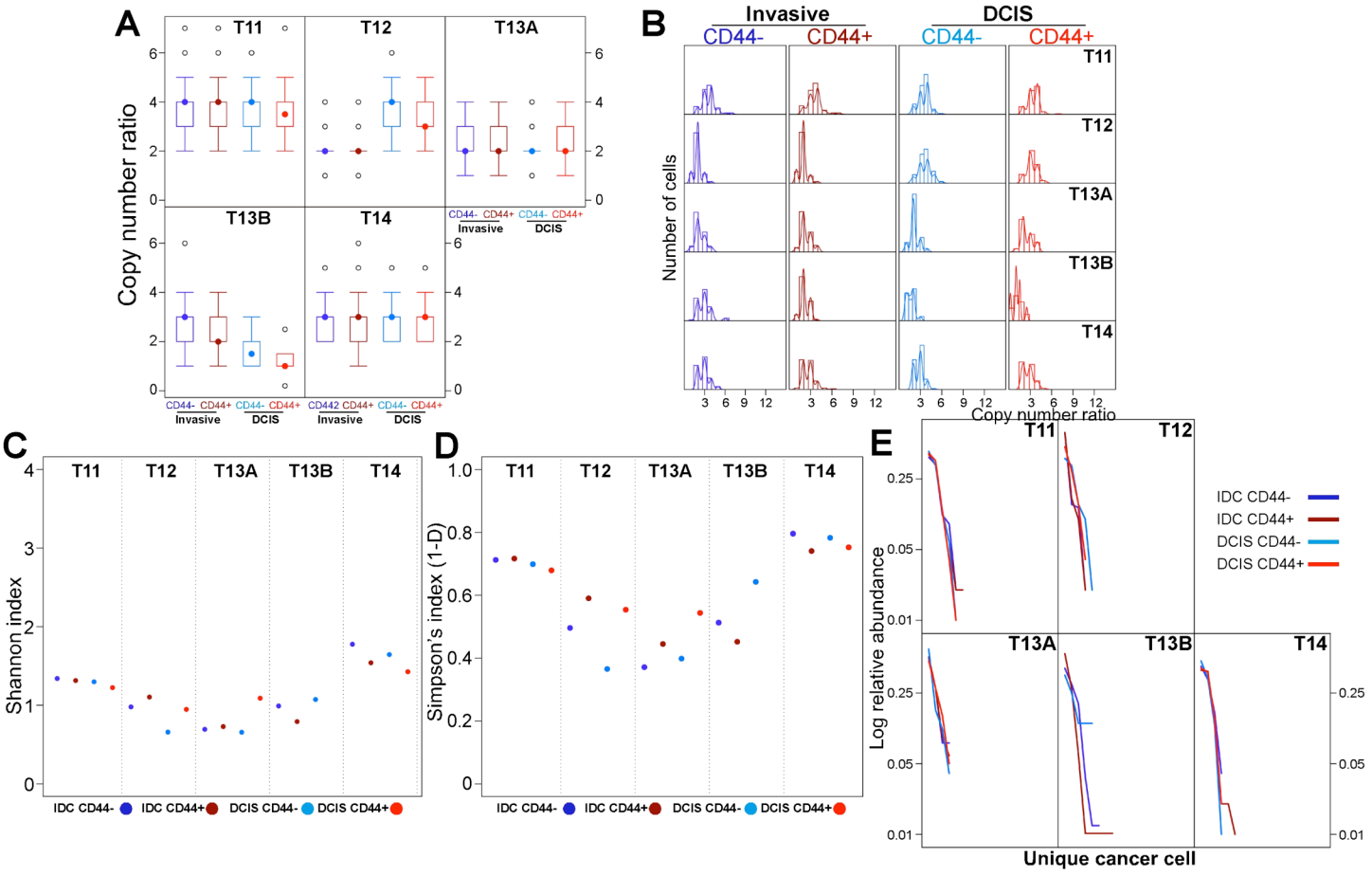

Supplemental Figure 9. Diversity of 16p13 copy number in luminal A breast tumors. (**A**) Box plot depicting the distribution of 16p13 copy number gain defined as the ratio of signal observed for the 16p13-specific and centromeric probes in 100 individual cells in each of the four indicated tumor cell subpopulations. Differences are seen between cell populations and also progression stages both for median copy number gain as well as for range of distribution. (**B**) Histograms and kernel density estimates depicting the distribution of cells with the indicated copy number ratio. (**C**) Shannon index depicting diversity within tumor cell subpopulations and tumors. Higher score indicates higher diversity. (**D**) Simpson's index depicting diversity within tumor cell subpopulations and tumors. Higher score indicates higher diversity. (**E**) Rank-abundance (Whittaker) plots depicting the abundance of unique cancer cells.

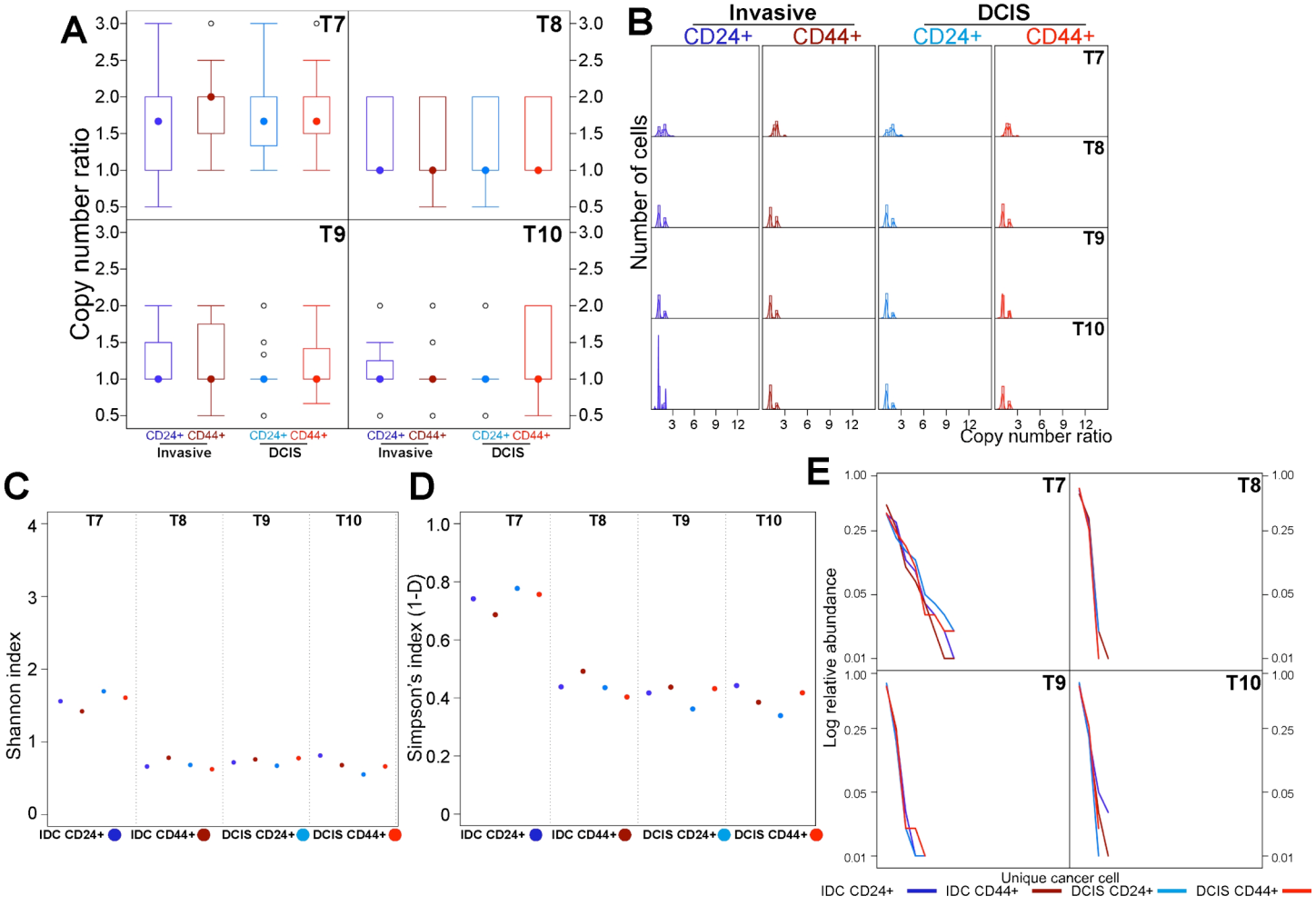

Supplemental Figure 10. Diversity of 17q21 copy number in HER2+ breast tumors. (**A**) Box plot depicting the distribution of 17q21 (ERBB2) copy number gain defined as the ratio of signal observed for the 17q21 specific and centromeric probes in 100 individual cells in each of the four indicated tumor cell subpopulations. Differences are seen between cell populations and also progression stages both for median copy number gain as well as for range of distribution. (**B**) Histograms and kernel density estimates depicting the distribution of cells with the indicated copy number ratio. In T6 the DCIS area lacked CD24+ cells. (**C**) Shannon index depicting diversity within tumor cell subpopulations and tumors. Higher score indicates higher diversity. (**D**) Simpson's index depicting diversity within tumor cell subpopulations and tumors. Higher score indicates higher diversity. (**E**) Rank-abundance (Whittaker) plots depicting the abundance of unique cancer cells.

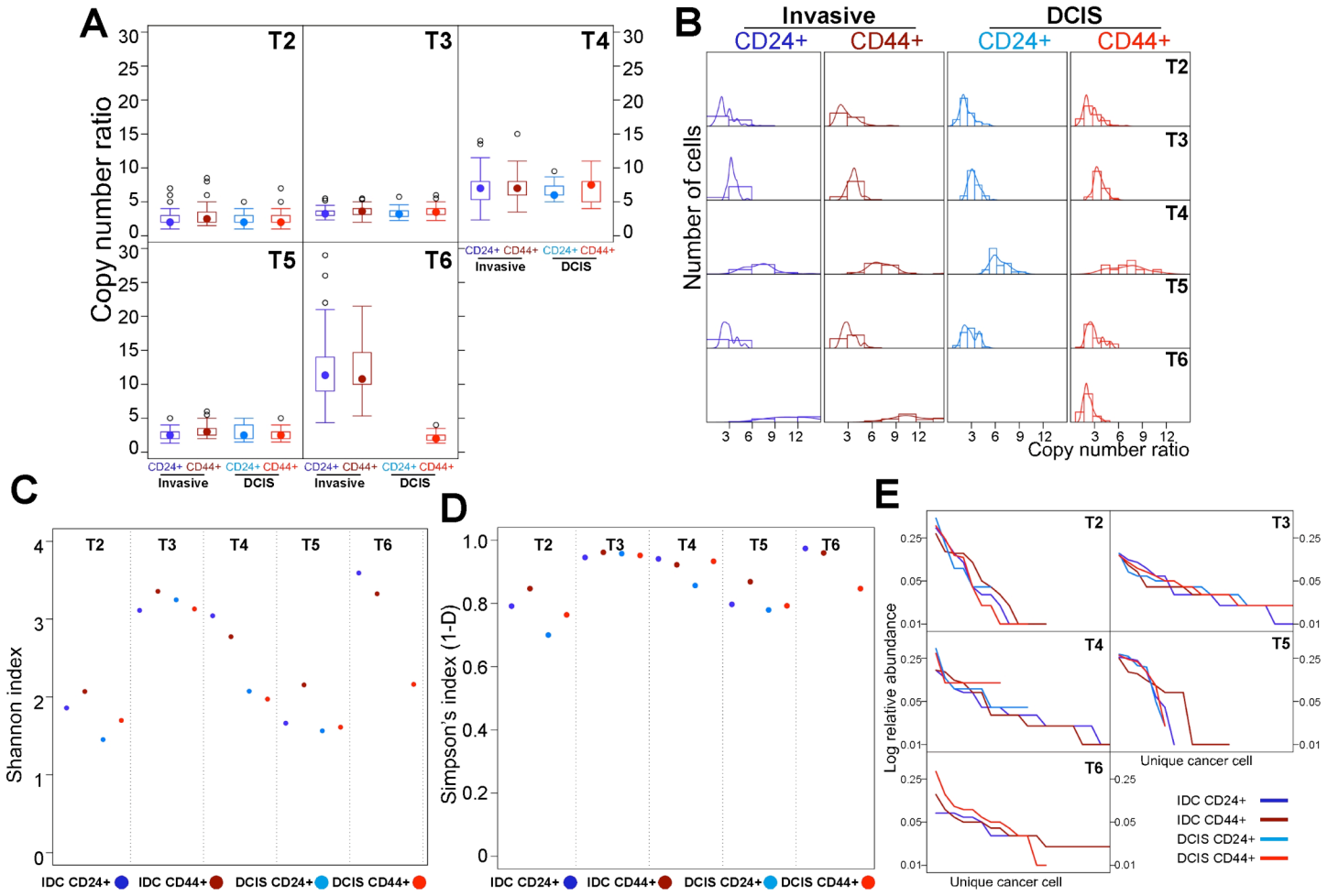

Supplemental Figure11. Bivariate scatter plots of the Shannon index for the 8q24 probe. The Shannon indices of CD44+ and CD24+ cell populations within the invasive areas are denoted by s1 and s2 and within DCIS by s3 and s4. Each plot depicts a pair of Shannon indices, as indicated by the diagonal entry. Hence the vertical axis of the first row of plots is s1 and also the horizontal axis of the first column is s1. For example, the scatter plot in the second row and first column depicts s1 on the horizontal axis and s2 on the vertical axis. No associations were detected.

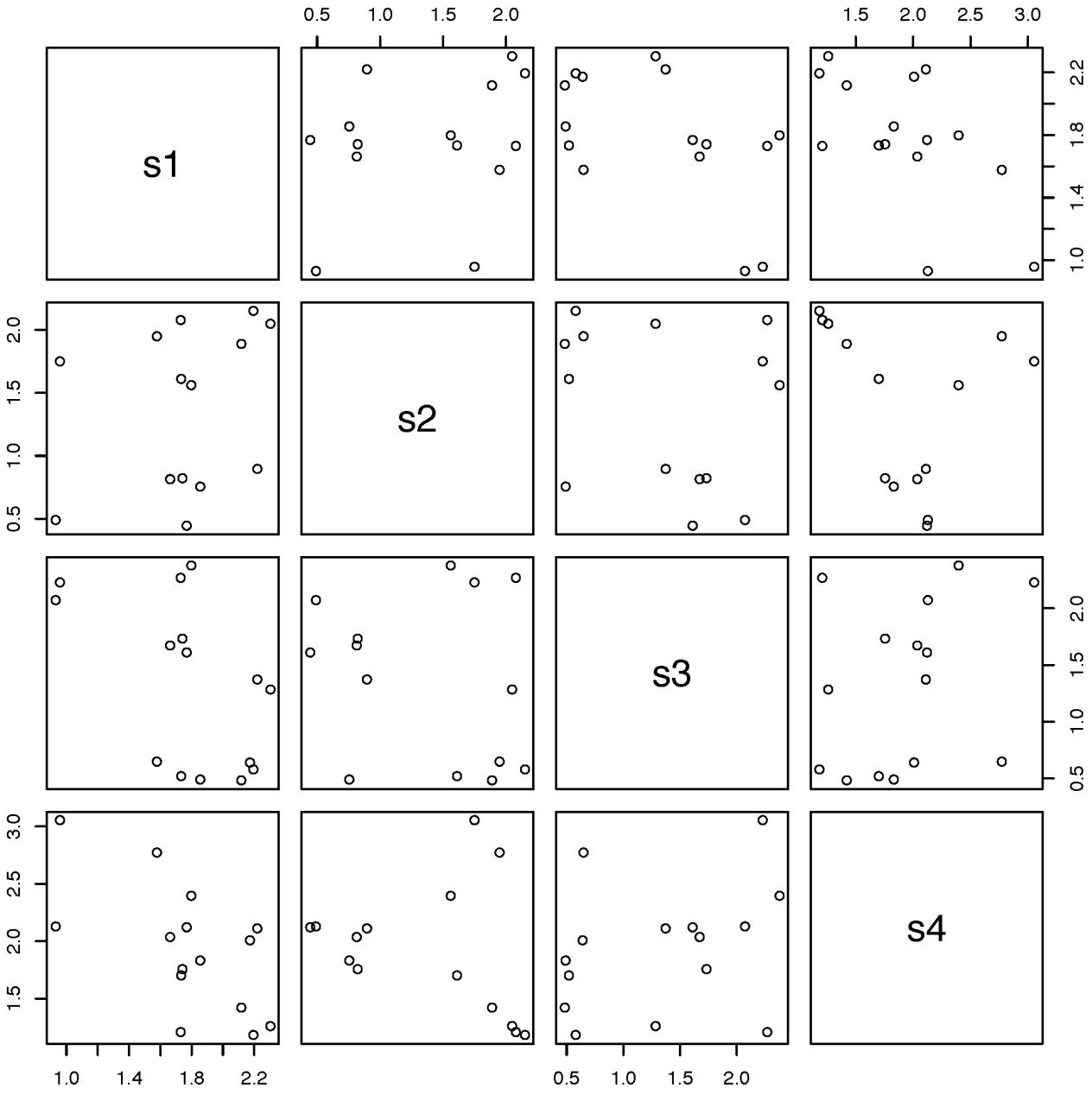

Supplemental Figure 12. Simpson's index for the 8q24 probe. (**A**) Simpson's index depicting diversity within tumor cell subpopulations and tumors. Higher score indicates higher diversity. (**B**) Hierarchical clustering of tumor samples based on Simpson's index for the 8q24 probe. The two dendrograms show how the tumors and cell types are clustered based on their Simpson's indices. Heatmap depicting the relatedness of the samples. Red and yellow indicate high and low diversity, respectively, whereas white represents median levels. Tumor names are colored according to subtype: red – basal-like, pink – HER2+, and blue – luminal A. Color key code indicates the correlation between diversity and colors.

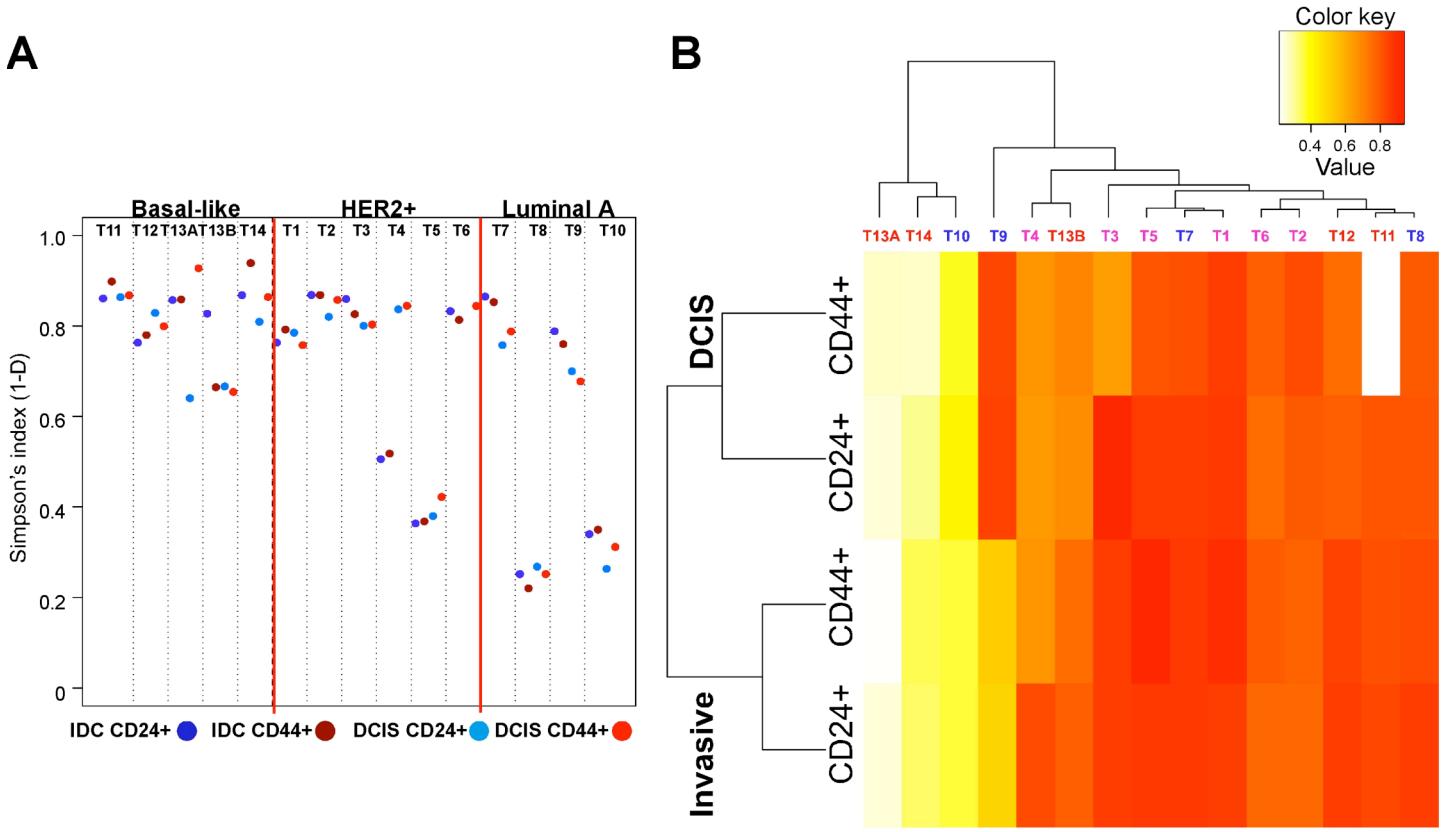

Supplemental Figure 12. Simpson's index for the 8q24 probe. (**A**) Simpson's index depicting diversity within tumor cell subpopulations and tumors. Higher score indicates higher diversity. (**B**) Hierarchical clustering of tumor samples based on Simpson's index for the 8q24 probe. The two dendrograms show how the tumors and cell types are clustered based on their Simpson's indices. Heatmap depicting the relatedness of the samples. Red and yellow indicate high and low diversity, respectively, whereas white represents median levels. Tumor names are colored according to subtype: red – basal-like, pink – HER2+, and blue – luminal A. Color key code indicates the correlation between diversity and colors.

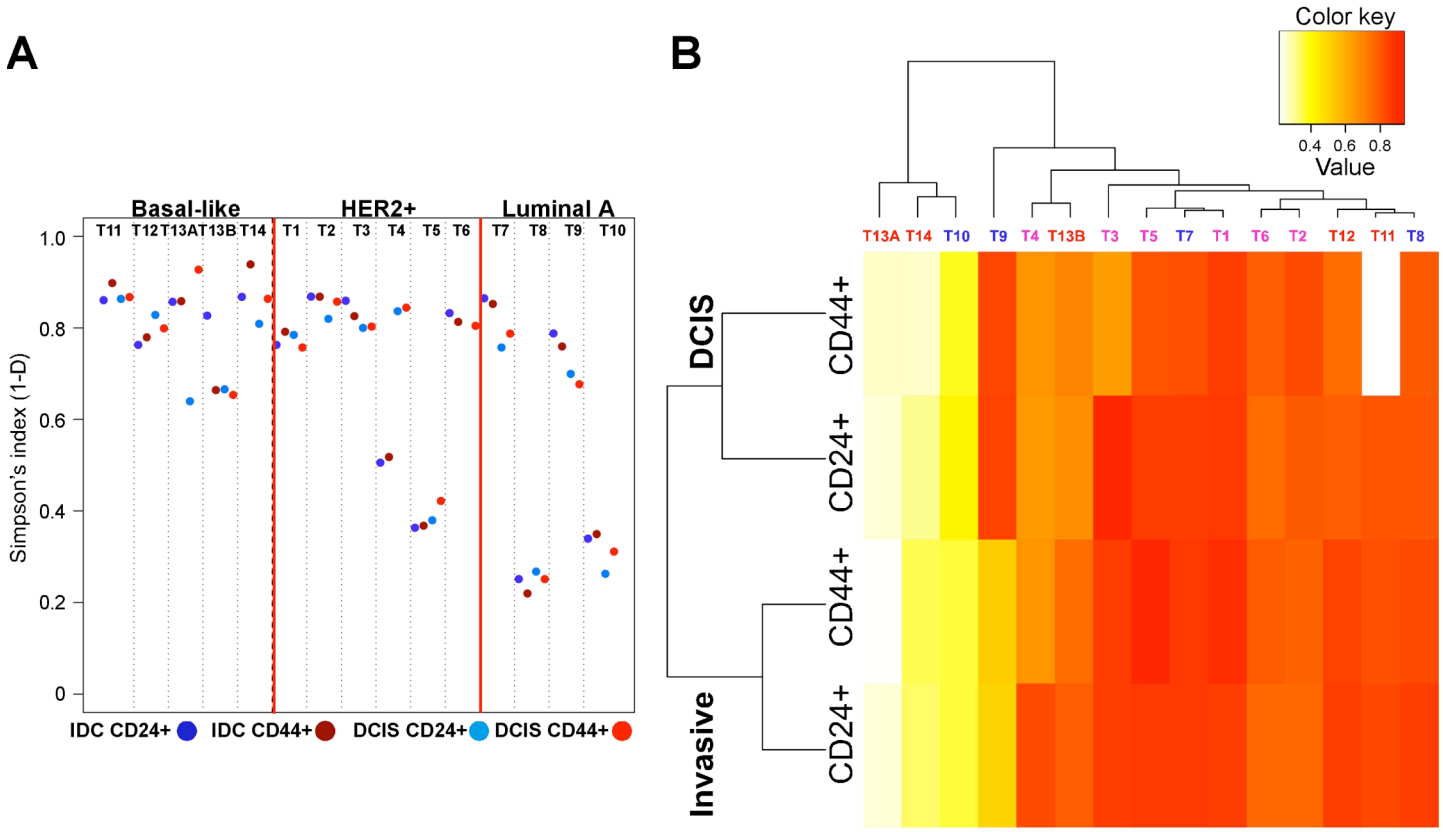

Supplemental Table 1. Histo-pathologic data of tumors. Tumor subytype, tumor size (in cm), pT and pN stage, histologic grade of IDC (tubule formation, nuclear pleomorphism, mitotic count), presence of intra-tumoral or preitumoral DCIS, nuclear grade of DCIS, extensive intraductal component (EIC), estrogen receptor (ER), progesteron receptor (PR), HER2, p53, and Ki-67 staining results are indicated. In columns marked with *, 0 and 1 correspond to lack and presence of the characteristics listed. For ER, PR, and p53, staining in more than 10% of the tumor cells was defined as positive. HER-2 staining was evaluated according to Hercept test grading criteria.

Subtype	Tumor #	Age	Size	pT stage	pN stage	Histologic grade of IDC	Tubule formation IDC	Nuclear pleomorphism IDC	Mitotic count IDC	intratumoral DCIS*	peritumoral DCIS*	Nuclear grade of DCIS	DCIS necrosis*	EIC*	ER*		PR*		HER2		p53*		Ki-67 (%)	
															DCIS	IDC	DCIS	IDC	DCIS	IDC	DCIS	IDC	DCIS	IDC
HER2+	T1	57	1.5	1	0	3	3	3	3	1	0	3	1	0	0	0	0	0	3	3	0	0	15	20
	T2	53	2.2	2	0	3	3	3	3	0	1	3	1	0	0	0	0	0	2	2	1	1	30	50
	T3	48	1.8	1	0	3	2	3	3	1	1	3	1	0	0	0	0	0	3	3	1	1	20	20
	T4	39	2.5	2	0	3	3	3	3	0	1	3	1	0	0	0	0	0	3	3	1	1	20	50
	T5	66	2.5	2	0	3	3	2	3	1	0	2	1	0	0	0	0	0	2	3	0	0	10	10
	T6	67	3	2	1	3	3	3	3	1	0	3	1	0	0	0	0	0	2	3	1	1	30	30
Luminal A	T7	56	2.5	2	0	2	2	2	2	1	1	2	1	0	1	1	1	1	1	1	0	0	5	5
	T8	48	1.3	1	1	2	3	2	1	1	1	2	0	0	1	1	1	1	1	1	0	0	2	5
	T9	58	1.9	1	0	1	2	1	1	1	1	1	0	0	1	1	1	1	0	0	0	0	3	3
	T10	54	1.5	1	0	2	2	2	3	0	1	2	0	0	1	1	1	1	1	1	0	0	2	30
Basal-like	T11	28	0.9	1	0	3	2	3	3	1	1	3	1	1	0	0	0	0	0	0	0	0	40	40
	T12	64	1	1	0	3	3	3	2	0	1	3	1	0	0	0	0	0	0	0	0	0	30	50
	T13A	40	0.8	1	1	3	3	3	3	1	1	3 & 2	1	0	0	0	0	0	0	0	**1**	**1**	50	50
	T13B	40	1.7	1	1	3	3	3	3	1	1	3	1	0	0	0	0	0	0	0	**1**	**1**	50	20
	T14	40	1.9	1	0	3	3	3	3	1	1	3	1	0	0	0	0	0	0	0	0	0	20	60

Supplemental Table 2. Topological diversity of tumors. Frequency of CD44+ and CD24+ cells in four independent quadrants of each tumor determined based on immunohistochemistry. In basal-like tumors (cases T11-14), CD24+ indicate CD44- cells. Frequencies (%) of tumor cells positive for CD24 and CD44 in four independent regions of invasive and *in situ* areas of the same tumor are listed.

Tumor	IDC													DCIS											
	area 1		area 2		area 3		area 4		Total		Distribution		CD44+/CD24+ pattern	area 1		area 2		area 3		area 4		Total		Distribution		CD44+/CD24+ pattern
	CD44+ (%)	CD24+ (%)	CD44+ (%)	CD24+ (%)	CD44+ (%)	CD24+ (%)	CD44+ (%)	CD24+ (%)	CD44+ (%)	CD24+ (%)	CD44+	CD24+*		CD44+ (%)	CD24+ (%)	CD44+ (%)	CD24+ (%)	CD44+ (%)	CD24+ (%)	CD44+ (%)	CD24+ (%)	CD44+ (%)	CD24+ (%)	CD44+	CD24+	
T1	95	20	95	30	90	10	85	50	95	25	diffuse	diffuse scattered/focally localized at the periphery	mixed	95	60	95	30					95	50	diffuse	diffuse	mixed
T2	80	30	25	25	70	30	50	35	30	40	diffuse scattered/focally localized at the periphery	diffuse scattered	mixed	70	20	90	0					80	5	diffuse	focally localized	mixed
T3	60	1	10	60	50	30	30	1	40	10	diffuse scattered	focally localized	separated	50	1	80	20					70	10	diffuse	focally localized	mixed
T4	60	5	50	5	5	50	0	50	10	20	focally localized	diffuse scattered	separated	5	5	5	5					5	5	diffuse scattered	diffuse scattered	mixed
T5	90	1	70	2	30	10	40	7	80	5	diffuse	diffuse scattered	mixed	30	10	50	10					50	10	diffuse	diffuse scattered	mixed
T6	80	15	90	7	90	50	80	30	70	20	diffuse	diffuse scattered/focally localized at the periphery	mixed	30	0							30	0	diffuse scattered		
T7	40	1	70	0	5	50	2	70	20	60	focally localized	focally localized	separated	10	70	10	30	70	5			50	50	diffuse	diffuse	mixed
T8	5	7	30	5	50	5	70	10	50	5	focally localized	focally localized	mixed	80	20	80	10					80	10	diffuse	diffuse scattered	mixed
T9	95	7	95	10	95	5	100	20	95	5	diffuse	diffuse scattered	mixed	95	10	95	10					95	10	diffuse	diffuse scattered	mixed
T10	10	3	10	3	10	10	7	5	10	5	diffuse scattered	diffuse scattered	mixed	90	10	70	10					80	10	diffuse	diffuse scattered	mixed
T11	7	93	10	90	70	30	15	85	10	90	diffuse scattered/focally localized at the periphery	diffuse	mixed	90	10	10	90	90	10			70	30	diffuse	diffuse	mixed
T12	60	40	80	20	10	90	40	60	30	70	diffuse scattered/focally localized at the periphery	diffuse	mixed	20	80	90	10					50	50	diffuse	diffuse	mixed
T13A	85	15	95	5	65	35	50	50	90	10	diffuse	focally localized	mixed	100	0	50	50	100	0			80	20	diffuse	focally localized	separated
T13B	30	70	15	85	30	70	20	80	20	80	diffuse scattered	diffuse	mixed	20	80	40	60	60	40			60	40	diffuse	diffuse	mixed
T14	50	50	40	60	15	85	5	95	30	70	diffuse scattered/focally localized at the periphery	diffuse	mixed	0	100	0	100	30	70			10	90	focally localized	diffuse	separated

Supplemental Table 3. List of BAC probes used for immuno-FISH experiments. Chromosomal location, gene within the BAC, and BAC clone names are indicated. X marks the probe used for FISH experiments in each of the three tumor subtypes.

Chromosome	1q32.1	8q24.13	10p13	11q13.2-13.3	12p13	16p13.3	17q21
Gene	NUAK2	NSMCE2	ITGA8	CCND1	H2AFJ	MPFL	ERBB2
BAC clone	CTD-2376C7	RP11-621K8	RP11-19L14	RP11-300I6	RP11-911J12	RP11-728H8	
Luminal A		x		x		x	
HER2+	x	x					x
Basal-like		x	x		x		

Supplemental Table 6. Associations between cell type, histology, and tumor subtype for all probes. Distribution of copy number ratios across tumor subtypes, cell types, and histologies were compared using a hierarchical model: the model for probe 621K8 was β_0+ β_1*(tumor subtype="Basal-like)+ β_2*(tumor subtype="HER2+")+ β_3*(cell type="CD24")+ β_4*(tumor subtype= "Basal-like)*(cell type="CD24")+β_5*(tumor subtype="HER2+")*(cell type= "CD24")+ β_6*(Histology= "DICS")+ β_7*(tumor subtype="Basal-like)**(Histology= "DICS")+ β_8*(tumor subtype= "HER2+")**(Histology="DICS")+β_9*(cell type="CD24")*(Histology= "DICS")+ β_{10}**(tumor subtype="Basal-like)*(cell type= "CD24")*(Histology =DCIS)+ β_{11}*(tumor subtype="HER2+")*(cell type="CD24")*(Histology="DCIS"). We identified significant differences between CD44- and CD44+ cells in the DCIS portion of basal-like tumors (p-value=0.001) for 8q24 copy number gain, and between CD24+ and CD44+ cells in the IDC portion of HER2+ tumors (p=0.002) for 1q32 copy number gain. No other comparisons were significant. All p-values were adjusted for multiple testing using simulation-based re-sampling.

	Parameter	Estimate	Standard Error	Tumor Subtype	Histology	Cell Type	Mean
8q24	β_0	3.2929	1.0403	Basal-like	DCIS	CD44-	2.91707
	β_1	-0.2618	1.396			CD44+	3.05277
	β_2	-1.4158	1.343		IDC	CD44-	2.8954
	β_3	0.02167	0.07149			CD44+	3.0311
	β_4	-0.1357	0.1031	HER2+	DCIS	CD24+	1.76307
	β_5	-0.09485	0.0923			CD44+	1.89877
	β_6	-0.3004	1.3553		IDC	CD24+	1.7414
	β_7	0.7	1.8188			CD44+	1.8771
	β_8	0.6773	1.7499	Luminal A	DCIS	CD24+	3.17887
	β_9	-0.2754	0.1011			CD44+	3.31457
	β_{10}	-0.8192	0.146		IDC	CD24+	3.1572
	β_{11}	0.3123	0.1393			CD44+	3.2929
1q32	β_0	4.3117	0.3904	HER2+	DCIS	CD24+	3.3084
	β_1	-0.235	0.0595			CD44+	4.258
	β_2	-0.9496	0.507		IDC	CD24+	3.3621
	β_3	0.1813	0.09748			CD44+	4.3117
ERBB2	β_0	6.4049	2.2024		DCIS	CD24+	3.5056
	β_1	-0.3305	0.1368			CD44+	6.2962
	β_2	-2.7906	2.4453		IDC	CD24+	3.6143
	β_3	0.2218	0.2591			CD44+	6.4049
11q13	β_0	3.3196	2.0698	Luminal A	DCIS	CD24+	1.43336
	β_1	-0.08521	0.07017			CD44+	3.29606
	β_2	-1.8627	2.081		IDC	CD24+	1.4569
	β_3	0.06167	0.09923			CD44+	3.3196
16p13	β_0	1.4035	0.1139		DCIS	CD24+	1.33829
	β_1	-0.06146	0.03107			CD44+	1.366
	β_2	-0.02771	0.17		IDC	CD24+	1.37579
	β_3	0.02396	0.04394			CD44+	1.4035
12p13	β_0	1.1758	0.02474	Basal-like	DCIS	CD44-	1.21717
	β_1	0.05771	0.0316			CD44+	1.15964
	β_2	0.05753	0.03295		IDC	CD44-	1.23333
	β_3	-0.07387	0.04411			CD44+	1.1758
10p13	β_0	1.167	0.06239		DCIS	CD44-	1.184
	β_1	0.01954	0.02751			CD44+	1.15678
	β_2	0.02722	0.08756		IDC	CD44-	1.19422
	β_3	-0.02976	0.03798			CD44+	1.167

Supplementary Table 7. Pairwise Pearson's correlations between histo-pathologic variables and the Shannon index for the 8q24 probe. Shannon indices, labeled s1-s4, correspond to IDC CD44+, IDC CD24+, DCIS CD44+ and DCIS CD24+. Red and blue colored cells depict high positive (red) and negative (blue) correlations. Abbreviations are the same as in Supplemental Table 1.

	Age	Size	pT.stage	LN.mets	pN.stage	DCIS.Grade	IDC.Grade	Tubule.formation	Nuclear.pleomorphism	Mitotic.count	intratumoral.DCIS	peritumoral.DCIS	DCIS.necrosis	EIC	DCIS.ER	IDC.ER	DCIS.PR	IDC.PR	DCIS.c.ERB2	IDC.c.ERB2	DCIS.P53	IDC.P53	DCIS.ki67	IDC.ki67	Shannon index of IDC CD24+	Shannon index of IDC CD44+	Shannon index of DCIS CD24+	Shannon index of DCIS CD44+
Age	1.00	0.44	0.36	-0.10	-0.10	-0.34	-0.22	0.11	-0.36	-0.24	-0.11	-0.58	-0.13	-0.55	0.19	0.19	0.19	0.19	0.27	0.39	-0.20	-0.20	-0.45	-0.38	0.57	0.24	-0.45	-0.07
Size	0.44	1.00	0.83	-0.10	-0.10	-0.07	-0.02	0.09	-0.14	0.13	0.00	-0.42	0.18	-0.38	0.00	0.00	0.00	0.00	0.52	0.62	0.26	0.26	-0.31	-0.21	0.37	-0.22	-0.37	-0.14
pT stage	0.36	0.83	1.00	-0.11	-0.11	0.03	0.16	0.20	0.00	0.20	-0.21	-0.35	0.35	-0.19	-0.11	-0.11	-0.11	-0.11	0.49	0.58	0.29	0.29	-0.13	-0.02	0.25	-0.10	-0.25	0.09
LN mets	-0.10	-0.10	-0.11	1.00	1.00	0.08	0.08	0.43	0.15	-0.08	0.36	-0.08	-0.08	-0.16	0.02	0.02	0.02	0.02	-0.23	-0.15	0.43	0.43	0.43	-0.11	-0.29	0.05	0.22	0.21
pN stage	-0.10	-0.10	-0.11	1.00	1.00	0.08	0.08	0.43	0.15	-0.08	0.36	-0.08	-0.08	-0.16	-0.02	-0.02	-0.02	-0.02	-0.23	-0.15	0.43	0.43	0.43	-0.11	-0.29	0.05	0.22	0.21
DCIS Grade	-0.34	-0.07	0.03	0.08	0.08	1.00	0.91	0.44	1.00	0.70	-0.18	-0.08	0.76	0.19	-0.83	-0.83	-0.83	-0.83	0.27	0.23	0.51	0.51	0.75	0.69	-0.45	-0.40	0.58	0.05
IDC Grade	-0.22	-0.02	0.16	0.08	0.08	0.91	1.00	0.55	0.91	0.79	-0.08	-0.28	0.84	0.15	-0.93	-0.93	-0.93	-0.93	0.29	0.32	0.46	0.46	0.67	0.61	-0.35	-0.47	0.61	0.18
Tubule formation	0.11	0.09	0.20	0.43	0.43	0.44	0.55	1.00	0.46	0.20	-0.11	-0.35	0.35	-0.38	-0.53	-0.53	-0.53	-0.53	0.12	0.18	0.29	0.29	0.35	0.37	-0.16	-0.49	0.20	0.35
Nuclear pleomorphism	-0.36	-0.14	0.00	0.15	0.15	1.00	0.91	0.46	1.00	0.71	-0.15	-0.05	0.76	0.17	-0.84	-0.84	-0.84	-0.84	0.21	0.17	0.53	0.53	0.73	0.71	-0.47	-0.36	0.59	0.14
Mitotic count	-0.24	0.13	0.20	-0.08	-0.08	0.70	0.79	0.20	0.71	1.00	-0.13	-0.28	0.66	0.15	-0.72	-0.72	-0.72	-0.72	0.34	0.36	0.46	0.46	0.51	0.53	-0.29	-0.35	0.37	-0.08
intratumoral DCIS	-0.11	0.00	-0.21	0.36	0.36	-0.18	-0.08	-0.11	-0.15	-0.13	1.00	-0.30	0.08	0.16	0.02	0.02	0.02	0.02	-0.16	-0.08	-0.12	-0.12	0.05	-0.50	-0.14	0.06	0.05	0.08
peritumoral DCIS	-0.58	-0.42	-0.35	-0.08	-0.08	-0.08	-0.28	-0.35	-0.05	-0.28	-0.30	1.00	-0.25	0.13	0.30	0.30	0.30	0.30	-0.49	-0.64	0.07	0.07	0.11	0.25	-0.38	-0.12	0.20	0.23
DCIS necrosis	-0.13	0.18	0.35	-0.08	-0.08	0.76	0.84	0.35	0.76	0.66	0.08	-0.25	1.00	0.13	-0.83	-0.83	-0.83	-0.83	0.23	0.26	0.41	0.41	0.62	0.45	-0.47	-0.43	0.55	0.37
EIC	-0.55	-0.38	-0.19	-0.16	-0.16	0.19	0.15	-0.38	0.17	0.15	0.16	0.13	0.13	1.00	-0.16	-0.16	-0.16	-0.16	-0.28	-0.27	-0.22	-0.22	0.31	0.15	-0.04	0.32	0.35	-0.37
DCIS ER	0.19	0.00	-0.11	-0.02	-0.02	-0.83	-0.93	-0.53	-0.84	-0.72	0.02	0.30	-0.83	-0.16	1.00	1.00	1.00	1.00	-0.23	-0.27	-0.49	-0.49	-0.72	-0.60	0.35	0.53	-0.64	-0.10
IDC ER	0.19	0.00	-0.11	-0.02	-0.02	-0.83	-0.93	-0.53	-0.84	-0.72	0.02	0.30	-0.83	-0.16	1.00	1.00	1.00	1.00	-0.23	-0.27	-0.49	-0.49	-0.72	-0.60	0.35	0.53	-0.64	-0.10
DCIS PR	0.19	0.00	-0.11	-0.02	-0.02	-0.83	-0.93	-0.53	-0.84	-0.72	0.02	0.30	-0.83	-0.16	1.00	1.00	1.00	1.00	-0.23	-0.27	-0.49	-0.49	-0.72	-0.60	0.35	0.53	-0.64	-0.10
IDC PR	0.19	0.00	-0.11	-0.02	-0.02	-0.83	-0.93	-0.53	-0.84	-0.72	0.02	0.30	-0.83	-0.16	1.00	1.00	1.00	1.00	-0.23	-0.27	-0.49	-0.49	-0.72	-0.60	0.35	0.53	-0.64	-0.10
DCIS ERB2	0.27	0.52	0.49	-0.23	-0.23	0.27	0.29	0.12	0.21	0.34	-0.16	-0.49	0.23	-0.28	-0.23	-0.23	-0.23	-0.23	1.00	0.97	0.33	0.33	0.28	-0.13	0.29	-0.21	-0.34	-0.21
IDC ERB2	0.39	0.62	0.58	-0.15	-0.15	0.23	0.32	0.18	0.17	0.36	-0.08	-0.64	0.26	-0.27	-0.27	-0.27	-0.27	-0.27	0.97	1.00	0.31	0.31	0.27	-0.17	0.38	-0.17	-0.31	-0.24
DCIS P53	-0.20	0.26	0.29	0.43	0.43	0.51	0.46	0.29	0.53	0.46	-0.12	0.07	0.41	-0.22	-0.49	-0.49	-0.49	-0.49	0.33	0.31	1.00	1.00	0.60	0.31	-0.43	-0.37	0.30	0.12
IDC P53	-0.20	0.26	0.29	0.43	0.43	0.51	0.46	0.29	0.53	0.46	-0.12	0.07	0.41	-0.22	-0.49	-0.49	-0.49	-0.49	0.33	0.31	1.00	1.00	0.60	0.31	-0.43	-0.37	0.30	0.12
DCIS Ki67	-0.45	-0.31	-0.13	0.43	0.43	0.75	0.67	0.35	0.73	0.51	0.05	0.11	0.62	0.31	-0.72	-0.72	-0.72	-0.72	-0.28	-0.27	0.60	0.60	1.00	0.55	-0.71	-0.20	0.76	0.24
IDC Ki67	-0.38	-0.21	-0.02	-0.11	-0.11	0.69	0.61	0.37	0.71	0.53	-0.50	0.25	0.45	0.15	-0.60	-0.60	-0.60	-0.60	-0.13	-0.17	0.31	0.31	0.55	1.00	-0.28	-0.26	0.49	0.13
Shannon index of IDC CD24+	0.57	0.37	0.25	-0.29	-0.29	-0.45	-0.35	-0.16	-0.47	-0.29	-0.14	-0.38	-0.47	-0.04	0.35	0.35	0.35	0.35	0.29	0.38	-0.43	-0.43	-0.71	-0.28	1.00	0.29	-0.56	-0.62
Shannon index of IDC CD44+	0.24	-0.22	-0.10	0.05	0.05	-0.40	-0.47	-0.49	-0.36	-0.35	0.06	-0.12	-0.43	0.32	0.53	0.53	0.53	0.53	-0.21	-0.17	-0.37	-0.37	-0.20	-0.26	0.29	1.00	-0.23	-0.26
Shannon index of DCIS CD24+	-0.45	-0.37	-0.25	0.22	0.22	0.58	0.61	0.20	0.59	0.37	0.05	0.20	0.55	0.35	-0.64	-0.64	-0.64	-0.64	-0.34	-0.31	0.30	0.30	0.76	0.49	-0.56	-0.23	1.00	0.30
Shannon index of DCIS CD44+	-0.07	-0.14	0.09	0.21	0.21	0.05	0.18	0.35	0.14	-0.08	0.08	0.23	0.37	-0.37	-0.10	-0.10	-0.10	-0.10	-0.21	-0.24	0.12	0.12	0.24	0.13	-0.62	-0.26	0.30	1.00